V European Conference on Computational Fluid Dynamics
ECCOMAS CFD 2010
J. C. F. Pereira and A. Sequeira (Eds)
Lisbon, Portugal,14-17 June 2010

APPLICATION OF RESPONSE SURFACE METHODOLOGY FOR MODELING AND OPTIMIZATION OF THE CYCLONE SEPARATOR FOR MINIMUM PRESSURE DROP

Khairy Elsayed*, Chris Lacor†

*Vrije Universiteit Brussel, Department of Mechanical Engineering,
Research Group Fluid Mechanics and Thermodynamics, Pleinlaan 2, B-1050 Brussels, Belgium,
e-mail: khairy.elsayed@vub.ac.be
†Vrije Universiteit Brussel, Department of Mechanical Engineering,
Research Group Fluid Mechanics and Thermodynamics, Pleinlaan 2, B-1050 Brussels, Belgium
e-mail: chris.lacor@vub.ac.be

Key words: Cyclone separator; Discrete phase modeling (DPM); Mathematical models; Response surface methodology (RSM); Design of experiment (DOE); Optimization

Abstract.

A Response surface design of experiment has been performed based on the Muschelknautz method of modeling (MM) for 64 test cases using Box-Behnken design to study the effect of seven geometrical cyclone dimensions on the pressure drop and cut-off diameter. It is found that the most significant geometrical parameters are, the vortex finder diameter, the inlet section width and height, and the cyclone total height. There are strong interactions between the effect of inlet dimensions and vortex finder diameter on the cyclone performance. CFD simulations based on Reynolds stress model are also used in the investigation. A new set of geometrical ratios (design) has been obtained (optimized) to achieve minimum pressure drop based on the Muschelknautz method of modeling. A comparison of numerical simulation of the new design and the Stairmand design confirms the superior performance of the new design compared to the Stairmand design.

1 Introduction

Cyclones are widely used in the air pollution control and gas–solid separation for aerosol sampling and industrial applications. With the advantages of relative simplicity to fabricate, low cost to operate, and well adaptability to extremely harsh conditions and high pressure and temperature environments, the cyclone separators have become one of the most important particle removal devices which are preferably utilized in scientific and engineering fields. Cyclones are frequently used as final collectors where large particles are to be caught. Efficiency is generally good for dusts where particles are larger than about 5 μm in diameter. They can also be used as pre-cleaners for a more efficient collector such as an electrostatic precipitator, scrubber or fabric filter.[1]

1.1 Cyclone performance

In addition to separation efficiency, pressure drop is considered as a major criterion to design cyclone geometry and evaluate cyclone performance. Therefore, an accurate mathematical model is needed to determine the complex relationship between pressure drop and cyclone characteristics. The pressure drop in a cyclone separator can also be decreased or increased by varying the cyclone dimensions. For an accurate optimal design of a cyclone, it is quite necessary to use a reliable pressure drop equation for it.

Currently, the pressure drop models for cyclone separators can be classified into three categories.[2] (1) the theoretical and semi-empirical models, (2) statistical models and (3) computational fluid dynamics (CFD) models.

The theoretical or semi-empirical models were developed by many researchers, e.g. Shepherd and Lapple,[3] Alexander,[4] First,[5] Stairmand,[6] Barth,[7] Avci and Karagoz,[8] Zhao,[9] Karagoz and Avci[10] and Chen and Shi.[11] These models were derived from physical descriptions and mathematical equations. They require a very detailed understanding of gas flow pattern and energy dissipation mechanisms in cyclones. In addition, due to using different assumptions and simplified conditions, different theoretical or semi-empirical models can lead to significant differences between predicted and measured results. Predictions by some models are twice more than experimental values and some models are even conflicted as to which models work best.[1]

In the 1980s, statistical models, as an alternative approach, were used to calculate cyclone pressure drop. For instance the models proposed by Casal and Martinez-Benet[12] and Dirgo[13] were developed through multiple regression analysis based on larger data sets of pressure drop for different cyclone configurations. Although statistical models are more convenient to predict the cyclone pressure drop, it is significantly more difficult to determine the most appropriate correlation function for fitting experimental data in this approach especially with the limited computer statistical softwares and robust algorithms available at that time.

Recently, the computational fluid dynamics (CFD) technique has presented a new way to model cyclone pressure drop. For instance, Gimbun et al.[14] successfully applied CFD to predict and to evaluate the effects of temperature and inlet velocity on the pressure drop of gas cyclones.[2] Undoubtedly, CFD is able to provide insight into the generation process of pressure drop across cyclones but additional research is still needed to have a good matching with experimental data. CFD is also computationally expensive in comparison with the mathematical models approach.

1.2 Stairmand design

In 1951 Stairmand[6] presented one of the most popular design guidelines which suggested that the cylinder height and the exit tube length should be, respectively, 1.5 and

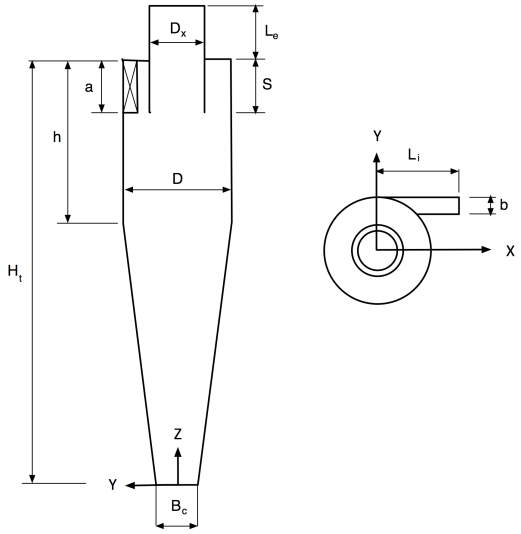

Figure 1: Schematic diagram for Stairmand cyclone separator

Table 1: The geometrical parameters values for Stairmand design (barrel diameter D=0.205 m)

Cyclone	a/D	b/D	D_x/D	H_t/D	h/D	S/D	B_c/D	L_i/D	L_e/D
Stairmand design	0.5	0.2	0.5	4	1.5	0.5	0.36	1.0	0.618

0.5 times of the cyclone body diameter for the design of a high efficiency cyclone[15] (Fig. 1 and Table 1). In the Stairmand model for pressure drop calculation,[16] the velocity distribution has been obtained from a moment-of-momentum balance, estimating the pressure drop as entrance and exit losses combined with the loss of static pressure in the swirl. The main drawbacks of the Stairmand model are: (1) Neglecting the entrance loss by assuming no change of the inlet velocity occurs at the inlet area. (2) Assuming constant friction factor. (3) The effect of particle mass loading on the pressure drop is not included. All these drawbacks are overcome in the **Muschelknautz Method** of modeling (MM)[17] introduced by Muschelknautz and Trefz.[18,19] The main benefit of MM over other models is its ability to take the following effects into account: a) wall roughness due to both the physical roughness of the materials of construction and to the presence of collected solids; b) the effect of mass loading and Reynolds number on cyclone performance; c) the change of flow velocity throughout the cyclone[17]

The present paper is an attempt to obtain a new optimized cyclone separator based on the MM model and to investigate the effect of each cyclone geometrical parameter on the cyclone performance using response surface methodology and CFD simulation.

1.3 The Muschelknautz method of modeling (MM)

Hoffmann and Stein[17] stated that, the most practical method for modeling cyclone separators at the present time is the Muschelknautz method (MM).[17,18,20–24] The roots of the Muschelknautz method (MM) extend back to the early work performed by Barth[7] as it is based on the equilibrium orbit model.[17]

1.3.1 The pressure loss in cyclone

According to MM model, the pressure loss across a cyclone occurs, primarily, as a result of friction with the walls and irreversible losses within the vortex core, the latter often dominating the overall pressure loss, $\Delta p = \Delta p_{body} + \Delta p_x$. In dimensionless form, it is defined as the Euler number.

$$E_u = \frac{1}{\frac{1}{2}\rho v_{in}^2} \left[\Delta p_{body} + \Delta p_x\right] \tag{1}$$

The wall loss, or the loss in the cyclone body is given by,

$$\Delta p_{body} = f \frac{A_R}{0.9\ Q} \frac{\rho}{2} \left(v_{\theta w} v_{\theta CS}\right)^{1.5} \tag{2}$$

where v_{in} is the area average inlet velocity, ρ is the gas density, Q is the gas volume flow rate, A_R is the total inside area of the cyclone contributing to frictional drag. The wall velocity, $v_{\theta w}$ is the velocity in the vicinity of the wall, and $v_{\theta cs}$ is the tangential velocity of the gas at the inner core radius.

The second contribution to pressure drop is the loss in the core and in the vortex finder is given by,

$$\Delta p_x = \left[2 + \left(\frac{v_{\theta cs}}{v_x}\right)^2 + 3\left(\frac{v_{\theta cs}}{v_x}\right)^{4/3}\right] \frac{1}{2}\ \rho v_x^2 \tag{3}$$

where v_x is the average axial velocity through the vortex finder (for more details refer to Hoffmann and Stein[17]).

1.3.2 Cut-off size

A very fundamental characteristic of any lightly loaded cyclone is its cut-point diameter or cut-off size x_{50} produced by the spin of the inner vortex. This is the practical diameter that has a 50% probability of capture. The cut size is analogous to the screen openings of an ordinary sieve or screen.[17] In lightly loading cyclone, x_{50} exercises a controlling influencing on the cyclone's separation performance. It is the parameter that determines the horizontal position of the cyclone grade-efficiency curve (fraction collected versus particle size). for low mass loading, the cut-off diameter can be estimated in MM via Eq.4.[17]

$$x_{50} = \sqrt{\frac{18\ \mu\ (0.9\ Q)}{2\ \pi\ (\rho_p - \rho) v_{\theta cs}^2 (H_t - S)}} \tag{4}$$

where μ is the gas dynamic viscosity, ρ_p is the particle density, H_t is the cyclone total height, and S is the vortex finder length.

2 Response surface methodology (RSM)

The cyclone separator performance and the flow field are affected mainly by the cyclone geometry where there are seven geometrical parameters, viz. inlet section height a and width b, vortex finder diameter D_x and length S, barrel height h, cyclone total height H_t and cone tip diameter B_c. all of these parameters are always expressed as a ratio of cyclone diameter D, as shown in Fig. 1 and Table 1.

The usual method of optimizing any experimental set-up is to adjust one parameter at a time, keeping all others constant, until the optimum working conditions are found. Adjusting one parameter at a time is necessarily time consuming, and may not reveal all interactions between the parameters. In order to fully describe the response and interactions of any complex system a multivariate parametric study must be conducted.[25] As there are seven geometrical parameters to be investigated, the best technique is to perform this study via the response surface methodology (RSM).

RSM is a powerful statistical analysis technique which is well suited to modeling complex multivariate processes, in applications where a response is influenced by several variables and the objective is to optimize this response. Box and Wilson first introduced the theory of RSM in 1951,[26] and RSM today is the most commonly used method of process optimization. Using RSM one may model and predict the effect of individual experimental parameters on a defined response output, as well as locating any interactions between the experimental parameters which otherwise may have been overlooked. RSM has been employed extensively in the field of engineering and manufacturing where many parameters are involved in a process.[27–29]

In order to conduct a RSM analysis, one must first design the experiment, identify the experimental parameters to adjust, and define the process response to be optimized. Once the experiment has been conducted and the recorded data tabulated, RSM analysis software models the data and attempts to fit second-order polynomial to this data.[25] The generalized second order polynomial model used in the response surface analysis was as follows:

$$Y = \beta_0 + \sum_{i=1}^{7} \beta_i X_i + \sum_{i=1}^{7} \beta_{ii} X_i^2 + \sum \sum_{i<j} \beta_{ij} X_i X_j \tag{5}$$

Table 2: The values of the independent variables

Variables	minimum	center	maximum
Inlet height, a/D =X1	0.4	0.55	0.7
Inlet width, b/D =X2	0.14	0.27	0.4
Vortex finder diameter, D_x/D =X3	0.2	0.475	0.75
Total cyclone height, H_t/D =X4	3.0	5.0	7.0
Cylinder height, h/D =X5	1.0	1.5	2.0
Vortex finder length, S/D =X6	0.4	1.2	2.0
Cone tip diameter, B_c/D =X7	0.2	0.3	0.4

where β_0, β_i, β_{ii}, and β_{ij} are the regression coefficients for intercept, linear, quadratic and interaction terms respectively. While X_i and X_j are the independent variables, and Y is the response variable (Euler number).

2.1 Design of experiment (DOE)

The statistical analysis is performed through three main steps. Firstly, construct a table of runs with combination of values of the independent variables via the commercial statistical software STATGRAPHICS centurion XV by giving the minimum and maximum values of the seven geometrical factors under investigation as input. Secondly, perform the runs by estimating the pressure drop (Euler number) using MM model. Thirdly, fill in the values of pressure drop in the STATGRAPHICS worksheet and obtain the response surface equation with main effect plot, interaction plots, Pareto chart and response surface plots beside the optimum settings for the new cyclone design.

Table 2 depicts the parameters ranges selected for the seven geometrical parameters. The study was planned using Box-Behnken design, with 64 combinations. A significant level of $P < 0.05$ (95% confidence) was used in all tests. Analysis of variance (ANOVA) was followed by an F-test of the individual factors and interactions.

2.2 Fitting the model

Analysis of variance (ANOVA) showed that the resultant quadric polynomial models adequately represented the experimental data with the coefficient of multiple determination R^2 being 0.92848. This indicates that the quadric polynomial model obtained was adequate to describe the influence of the independent variables studied.[30] Analysis of variance (ANOVA) was used to evaluate the significance of the coefficients of the quadric polynomial models (see Table 3). For any of the terms in the models, a large F-value (small P-value) would indicate a more significant effect on the respective response variables.

Based on the ANOVA results presented in Table 3, the variable with the largest effect on

the pressure drop (Euler number) was the linear term of vortex finder diameter, followed by the linear term of inlet width and inlet height ($P < 0.05$); the other four linear terms (barrel height, vortex finder length, cyclone total height and cone-tip diameter) did not show a significant effect ($P > 0.05$). The quadric term of vortex finder diameter also had a significant effect ($P < 0.05$) on the pressure drop, however, the effect of the other six quadric terms was insignificant ($P > 0.05$). Furthermore, the interaction between the inlet dimensions and vortex finder diameters ($P < 0.05$) also had a significant effect on the pressure drop, while the effect of the remaining terms was insignificant ($P > 0.05$).

2.3 Analysis of response surfaces

For visualization of the calculated factor, main effects plot, pareto chart and response surface plots were drawn. The slope of the main effect curve is proportional to the size of the effect and the direction of the curve specifies a positive or negative influence of the effect[31](Fig.2(a)). Based on the main effect plot, the most significant factor on the Euler number are (1) the vortex finder diameter, with a second order curve with a wide range of inverse relation and a narrow range of direct relation, (2) direct relation with inlet dimensions, (3) inverse relation with cyclone total height and insignificant effects for the other factors.

Pareto charts were used to graphically summarize and display the relative importance of each parameter with respect to the Euler number. The Pareto chart shows all the linear and second-order effects of the parameters within the model and estimate the significance of each with respect to maximizing the Euler number response. A Pareto chart displays a frequency histogram with the length of each bar proportional to each estimated standardized effect.[25] The vertical line on the Pareto charts judges whether each effect is statistically significant within the generated response surface model; bars that extend beyond this line represent effects that are statistically significant at a 95% confidence level. Based on the Pareto chart (Fig. 2(b)) and ANOVA table (Table 3) there are four significant parameters (six terms in the ANOVA table) at a 95% confidence level: the negative linear vortex finder diameter; the linear inlet width; the linear total cyclone height; a second-order vortex finder diameter; negative interaction between vortex finder diameter and inlet dimensions. These are the major terms in a polynomial fit to the data. Therefore, the pareto chart is a perfect supplementation to the main effects plot.

To visualize the effect of the independent variables on the dependent ones, surface response of the quadric polynomial models were generated by varying two of the independent variables within the experimental range while holding the other factors at their central values.[30] Thus, Fig. 2(c) was generated by varying the inlet height and the inlet width while holding the other five factors, The trend of the curve is linear, with more significant effect for inlet width, with no interaction between the inlet height and width. The response surface plots given by Figs. 2(d), 2(e) and 2(f) show that, there are interactions between both inlet width and inlet height with the vortex finder diameter. The effect of cyclone total height is less significant with respect to the vortex finder diameter,

but its effect is higher than that of the vortex finder length, the barrel height and the cone tip diameter.

2.4 Optimization(Downhill Simplex method)

The Nelder-Mead method, also known as **downhill simplex method** is a commonly used nonlinear optimization technique, The technique was proposed by Nelder and Mead[32] and is a technique for minimizing an objective function in a many-dimensional space.[33] It requires only function evaluations, and no calculation of derivatives.[34]

Table 4 gives the optimum values for cyclone geometrical parameters for minimum pressure drop estimated by MM via Downhill Simplex optimization technique available in STATGRAPHICS software.

3 Comparison between the two designs using CFD

3.1 Numerical settings

For the turbulent flow in cyclones, the key to the success of CFD lies with the accurate description of the turbulent behavior of the flow.[35] To model the swirling turbulent flow in a cyclone separator, there are a number of turbulence models available in FLUENT. These range from the standard $k-\varepsilon$ model to the more complicated Reynolds stress model (RSM). Also Large eddy simulation (LES) is available as an alternative to the Reynolds averaged Navier-Stokes approach. The standard $k-\varepsilon$, RNG $k-\varepsilon$ and Realizable $k-\varepsilon$ models were not optimized for strongly swirling flows found in cyclones.[36] The Reynolds stress turbulence model (RSM) requires the solution of transport equations for each of the Reynolds stress components. It yields an accurate prediction on swirl flow pattern, axial velocity, tangential velocity and pressure drop in cyclone simulations.[37]

The air volume flow rate Q_{in}=0.0841 $[m^3/s]$ for the two cyclones (Inlet velocity for Stairmand design is 19[m/s] and 13.1[m/s] for the new design), air density 1.0 $[kg/m^3]$ and dynamic viscosity of 1.0E-5$[Pa\ s]$. the turbulent intensity equals 5% and characteristic length equals 0.07 times the inlet width.

The finite volume method has been used to discretize the partial differential equations of the model using the SIMPLEC (Semi-Implicit Method for Pressure-Linked Equations-Consistent) method for pressure velocity coupling and QUICK scheme to interpolate the variables on the surface of the control volume. The implicit coupled solution algorithm was selected. The unsteady Reynolds stress turbulence model (RSM) was used in this study with a time step of 0.001 [s]. The residence time (cyclone volume/gas volume flow rate) of the two cyclones are close ($\approx$ 0.25[s]).

The numerical grid of the Stairmand cyclone contains 134759 hexahedral cells while 154746 hexahedral cells are used for the new design. The simulations were performed on

Table 3: Analysis of variance of the regression coefficients of the fitted quadratic equation*

Variable	Regression coefficient	F-Ratio	P-Value
β_0	-43.0742		
Linear			
β_1	178.176	8.11	**0.0075**
β_2	372.26	19.79	**0.0001**
β_3	-161.452	232.04	**0.0000**
β_4	-1.55344	0.6	0.446
β_5	8.5875	0	0.9691
β_6	-7.23112	0.1	0.757
β_7	19.5663	0	0.9537
Quadric			
β_{11}	1.08238	0	0.9931
β_{22}	-12.2111	0	0.9446
β_{33}	403.419	107.8	**0.0000**
β_{44}	-0.223597	0.09	0.7641
β_{55}	-2.67108	0.05	0.8223
β_{66}	1.81257	0.15	0.6994
β_{77}	-62.1739	0.04	0.8364
Interaction			
β_{12}	91.0488	0.22	0.6427
β_{13}	-355.892	14.75	**0.0005**
β_{14}	0.459314	0	0.9726
β_{15}	-3.27883	0	0.9514
β_{16}	2.19997	0	0.9465
β_{17}	26.2787	0.01	0.9191
β_{23}	-720.685	42.42	**0.0000**
β_{24}	1.03571	0	0.9467
β_{25}	-2.53478	0	0.9675
β_{26}	4.2616	0.01	0.9112
β_{27}	-5.28466	0	0.9862
β_{34}	5.2034	0.51	0.4799
β_{35}	2.77536	0.01	0.9249
β_{36}	0.985086	0	0.9568
β_{37}	32.579	0.05	0.8221
β_{45}	-0.0452174	0	0.9911
β_{46}	0.345301	0.02	0.8902
β_{47}	-1.5016	0.01	0.9404
β_{56}	-0.422227	0	0.9667
β_{57}	3.82354	0	0.9622
β_{67}	-6.40134	0.02	0.8945
R^2	0.92848		

* Bold numbers indicate significant factors as identified by the analysis of variance (ANOVA) at the 95% confidence level.

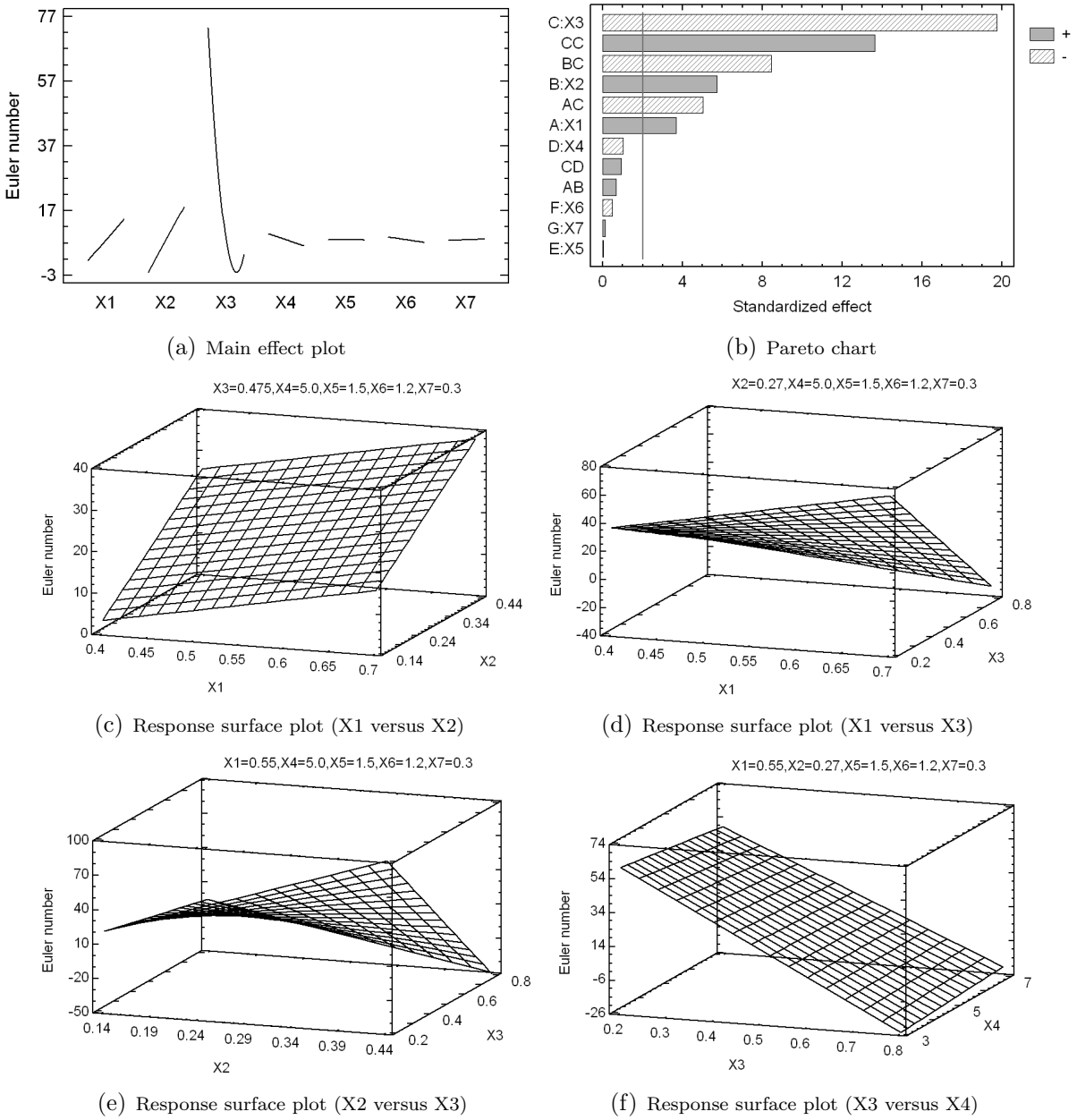

(a) Main effect plot

(b) Pareto chart

(c) Response surface plot (X1 versus X2)

(d) Response surface plot (X1 versus X3)

(e) Response surface plot (X2 versus X3)

(f) Response surface plot (X3 versus X4)

Figure 2: Analysis of design of experiment

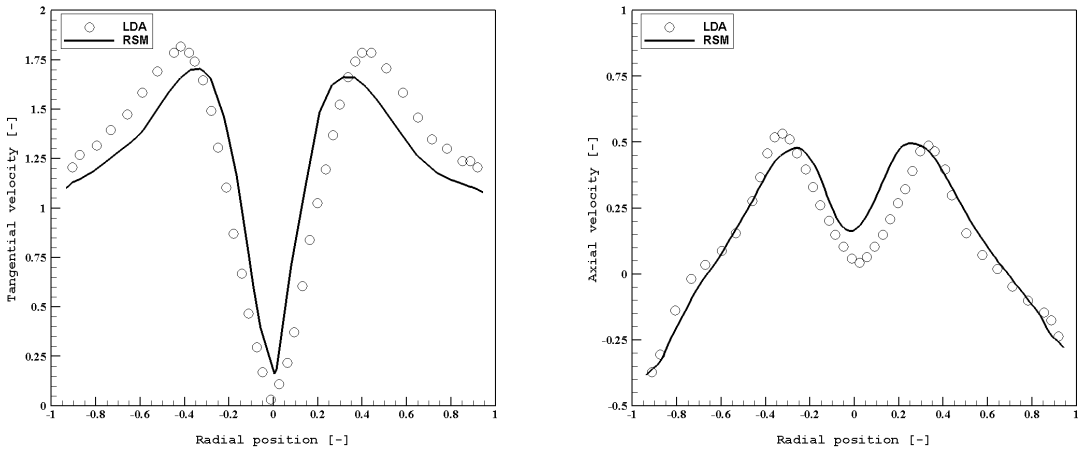

Figure 3: Comparison of the time averaged tangential and axial velocity between the LDA measurements, Hoekstra[38] and the current Reynolds stress model (RSM) results at section S6. From left to right tangential velocity and axial velocity, D_x/D=0.5.

an 8 nodes CPU Opteron 64 Linux cluster. The geometrical values are given in Table 5 for the two cyclones (cf. Fig. 1)

4 Results and discussion

4.1 Validation of results

In order to validate the obtained results, it is necessary to compare the prediction with experimental data. The comparison performed with the the measurements of Hoekstra[38] of the Stairmand cyclone using Laser Doppler Anomemetry (LDA). The present simulation are compared with the measured axial and tangential velocity profiles at an axial station located at 94.25 cm from the cyclone bottom ($D_x/D = 0.5$), Fig. 3. The RSM simulation matches the experimental velocity profile with underestimation of the maximum tangential velocity, and overestimation of the axial velocity at the central region. Considering the complexity of the turbulent swirling flow in the cyclones, the agreement between the simulations and measurements is considered to be quite acceptable.

Table 4: Optimize response for minimum pressure drop

Factor	Low	High	Optimum
X1	0.5	0.75	0.618025
X2	0.14	0.4	0.23631
X3	0.2	0.75	0.621881
X4	3	7	4.23618
X5	1.618	1.618	1.618
X6	0.4	2	0.620421
X7	0.2	0.4	0.381905

4.2 Flow field pattern

4.2.1 The pressure field

Figure 4 shows the contour plot at Y=0 and at section S7 (at the middle of inlet section, Table 6). In the two cyclones the time-averaged static pressure decreases radially from wall to center. A negative pressure zone appears in the forced vortex region (central region) due to high swirling velocity. The pressure gradient is largest along the radial direction, while the gradient in axial direction is very limited. The cyclonic flow is not symmetrical as is clear from the shape of the low pressure zone at the cyclone center (twisted cylinder). However the two cyclones have almost the same flow pattern, but the highest pressure of the Stairmand design is nearly twice that of the new design, implying that the new design has a lower pressure drop.

The pressure distribution presented in Figs. 5 and 6 of the two cyclones at sections S1 till S6 depict the two parts pressure profile (for Rankine vortex). Again the highest static pressure for Stairmand design is more than twice that of the new design at all sections while the central value is almost the same for the two cyclones irrespective to the section location. This indicates that, the new design has a lower pressure drop with respect to the Stairmand design.

4.2.2 The velocity field

Based on the contour plots of the time averaged tangential velocity, Fig 4, and the radial profiles at sections S1 through S6 shown in Figs. 5 and 6, the following comments can be drawn. The tangential velocity profile at any section is composed of two regions, an inner and an outer one. In the inner region the flow rotates approximately like a solid body (forced vortex), where the tangential velocity increases with radius. After reaching its peak the velocity decreases with radius in the outer part of the profile (free vortex). This profile is a so-called Rankine type vortex as mentioned before, including a quasi-forced vortex in the central region and a quasi-free vortex in the outer region. The maximum tangential velocity may reach twice the average inlet velocity and occurs in the annular cylindrical part. The tangential velocity distribution for the two cyclones are nearly identical in pattern and values (dimensionless), with the highest velocity occurring

Table 5: The values of geometrical parameters for the two designs (D=0.205 m)

Cyclone	a/D	b/D	D_x/D	H_t/D	h/D	S/D	B_c/D	L_i/D	L_e/D
Stairmand design	0.5	0.2	0.5	4	1.5	0.5	0.36	1.0	0.618
New design	0.618	0.236	0.618	4.236	1.618	0.618	0.382	1.0	1.618

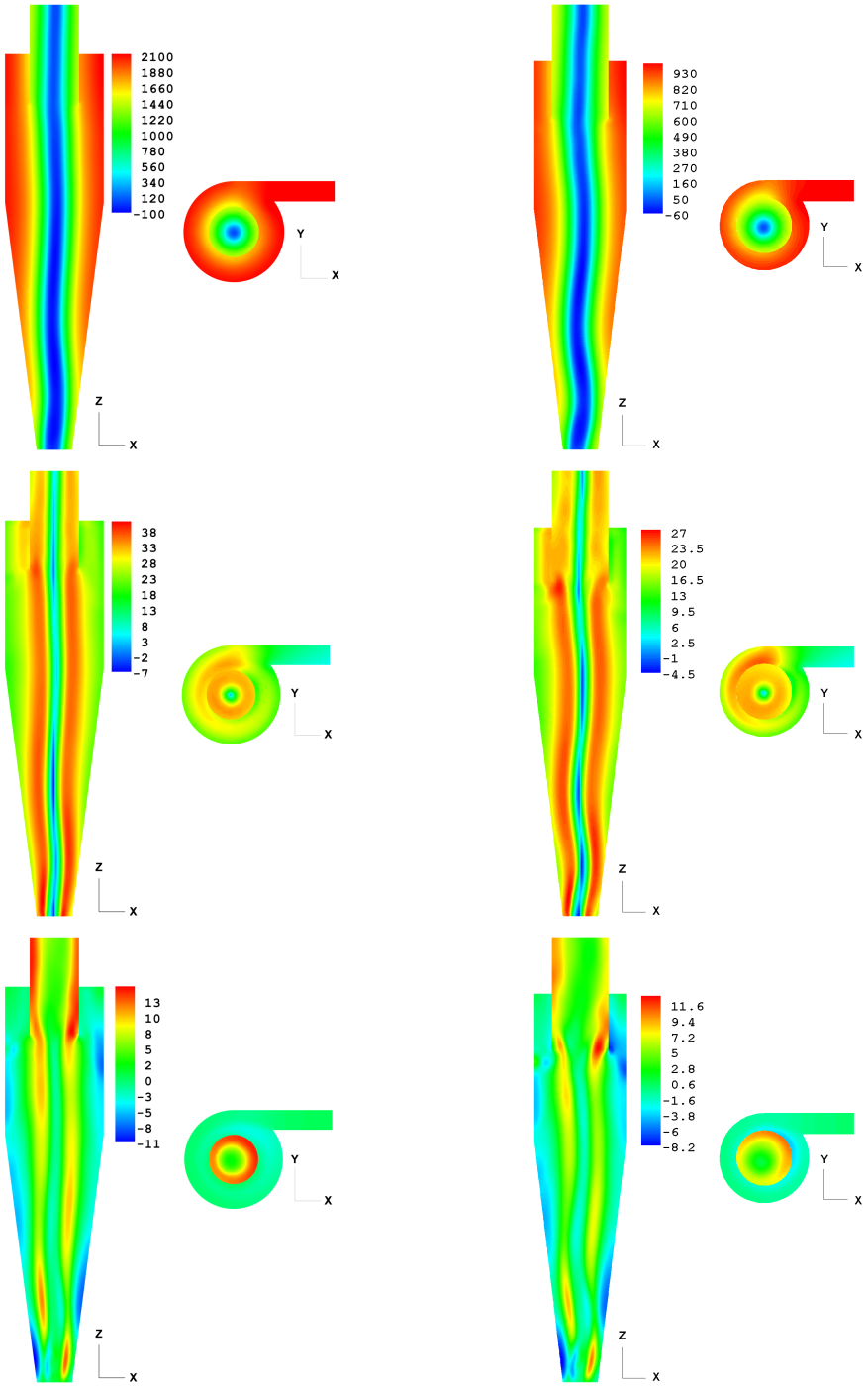

Figure 4: The contour plots for the time averaged flow variables at sections Y=0 and S7. From top to bottom: static pressure [N/m^2], tangential velocity [m/s] and axial velocity [m/s]. From left to right Stairmand design and new design respectively.

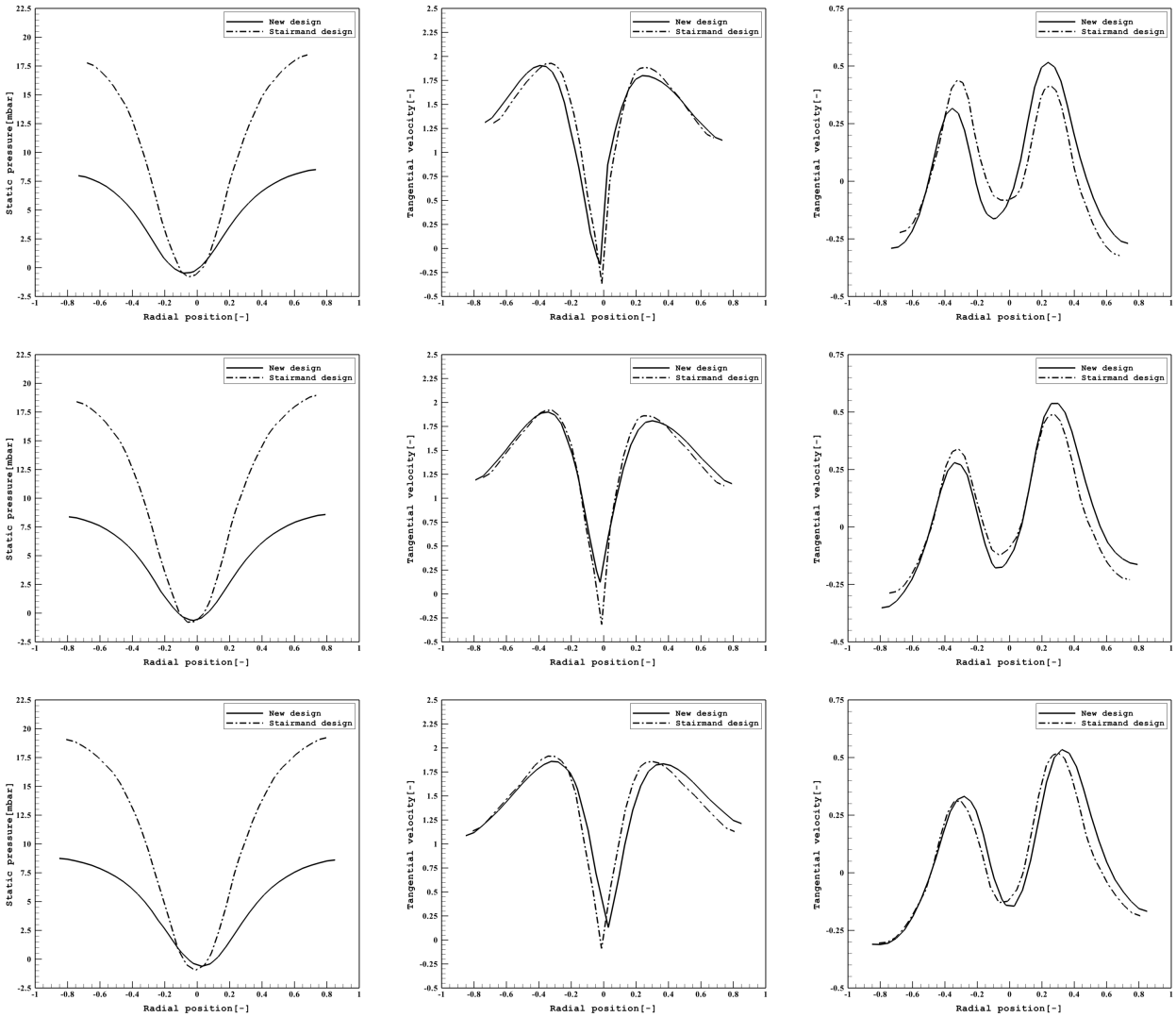

Figure 5: The radial profile for the time averaged tangential and axial velocity at different sections on the X-Z plane (Y=0) at sections S1 till S3 . From top to bottom: section S1 through section S3. From left to right: time-averaged static pressure, tangential velocity and axial velocity respectively.

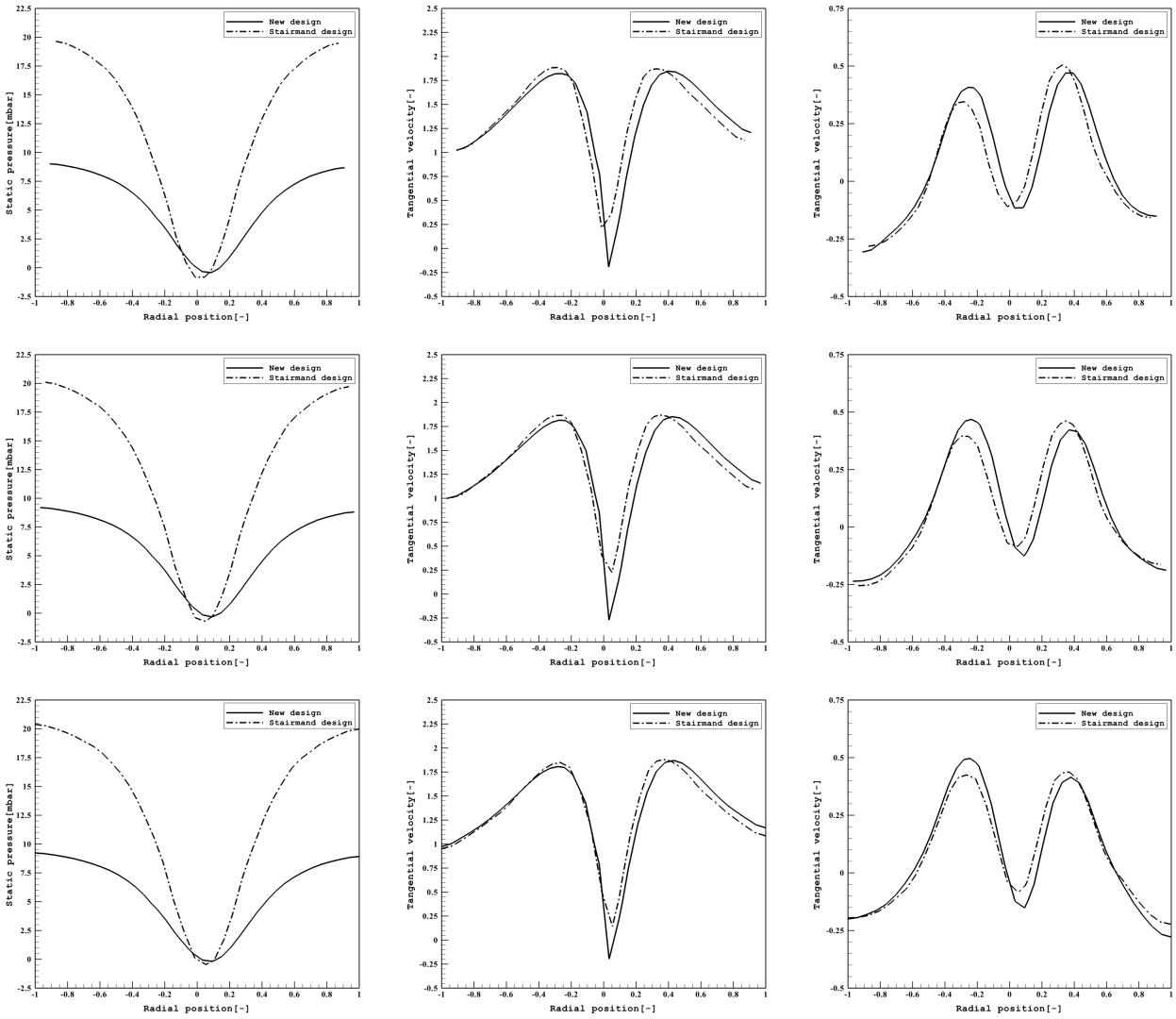

Figure 6: The radial profile for the time averaged tangential and axial velocity at different sections on the X-Z plane (Y=0) at sections S4 till S6 . From top to bottom: section S4 through section S6. From left to right: time-averaged static pressure, tangential velocity and axial velocity respectively.

Table 6: The position of different sections[§]

Section	S1	S2	S3	S4	S5	S6	S7
z'/D[†]	2.75	2.5	2.25	2.0	1.75	1.5	0.25

[§] Sections S1 through S5 are located in the conical section, section S6 at the cylindrical part and S7 located through the inlet section.
[†] z' measured from the inlet section top

at 1/4 of the cyclone radius for both cyclones. This implies a nearly equal collection efficiency for both cyclones, as the centrifugal force is the main driving force for particle collection in the cyclone separator. The axial velocity profiles for the two cyclones are also very close, exhibiting a M letter shape (also known as inverted W axial velocity profile in some other literatures (cf. Horvath et al.[39])). Based on the flow pattern analysis one can conclude that, the cyclone collection efficiency for the two cyclones should be very close, with the advantage of low pressure drop in the new design. The authors want to emphasis that only small changes in the geometrical dimensions of the two designs lead to this improvement in the performance.

4.3 Discrete phase modeling (DPM)

The Lagrangian discrete phase model in FLUENT follows the Euler-Lagrange approach. The fluid phase is treated as a continuum by solving the time-averaged Navier-Stokes equations, while the dispersed phase is solved by tracking a large number of particles through the calculated flow field. The dispersed phase can exchange momentum, mass, and energy with the fluid phase.

A fundamental assumption made in this model is that the dispersed second phase occupies a low volume fraction (usually less than 10–12 %, where the volume fraction is the ratio between the total volume of particles and the volume of fluid domain), even though high mass loading is acceptable. The particle trajectories are computed individually at specified intervals during the fluid phase calculation. This makes the model appropriate for the modeling of particle-laden flows. The particle loading in a cyclone separator is small (3-5 %), and therefore, it can be safely assumed that the presence of the particles does not affect the flow field (one-way coupling).

In FLUENT, the drag coefficient for spherical particles is calculated by using the correlations developed by Morsi and Alexander.[40] The equation of motion for particles was integrated along the trajectory of an individual particle. Collection efficiency statistics were obtained by releasing a specified number of mono-dispersed particles at the inlet of the cyclone and by monitoring the number escaping through the outlet. Collisions between particles and the walls of the cyclone were assumed to be perfectly elastic (coefficient of restitution is equal to 1).

Table 7: The Euler number E_u, pressure drop Δp and the cut-off diameter (x_{50}) for the two cyclones

	Method	E_u [-]	Δp $[N/m^2]$	X_{50} $[\mu m]$
Stairmand design	MM	5.79	1045	1.54
	CFD	6.592	1190	1.0
New design	MM	5.24	450	1.77
	CFD	5.672	487	1.6

4.3.1 The DPM results

In order to calculate the cut-off diameters of the two cyclones, 5880 particles were injected from the inlet surface with zero velocity and a particles mass flow rate $\dot{m}_p$ of 0.001 $[kg/s]$ (corresponding to inlet dust concentration $C_{in}(\dot{m}_p/Q) = 11.891$ $[gm/m^3]$). The particle density ρ_p is 860 $[kg/m^3]$ and the maximum number of time steps for each injection was 200000 steps. The DPM analysis results and the pressure drops for the two cyclones are depicted in Table 7. A good matching between the CFD results and the MM mathematical model are obtained. While the difference between the two cyclone cut-off diameters is small, the saving in pressure drop is considerable (nearly half the value of Stairmand cyclone).

5 Conclusions

Mathematical modeling (the Muschelknautz method of modeling (MM)) and CFD investigation has been used to understand the effect of the cyclone geometrical parameters on the cyclone performance and a new optimized cyclone geometrical ratios based on MM model has been obtained.

The most significant geometrical parameters are: (1) the vortex finder diameter, (2) the inlet section width, (3) the inlet section height and (4) the cyclone total height. There are strong interaction between the effect of inlet dimensions and the vortex finder diameter on the cyclone performance. The new cyclone design are very close to the Stairmand high efficiency design in the geometrical parameter ratio, and superior for low pressure drop at nearly the same cut-off diameter. The new cyclone design results in nearly one-half the pressure drop obtained by the old Stairmand design at the same volume flow rate.

REFERENCES

[1] P. K. Swamee, N. Aggarwal, and K. Bhobhiya. Optimum design of cyclone separator. *American Institute of Chemical Engineers (AIChE)*, 55(9):2279–2283, 2009.

[2] B. Zhao. Modeling pressure drop coefficient for cyclone separators a support vector machine approach. *Chemical Engineering Science*, 64:4131–4136, 2009.

[3] C. B. Shepherd and C. E. Lapple. Flow pattern and pressure drop in cyclone dust collectors cyclone without intel vane. *Industrial & Engineering Chemistry*, 32(9): 1246–1248, September 1940.

[4] R. M. Alexander. Fundamentals of cyclone design and operation. In *Proceedings of the Australian Institute of Mineral and Metallurgy (New Series)*, 152–153, pages 203–228, 1949.

[5] M. W. First. Cyclone dust collector design. *ASME Annual General Meeting, Paper no. 49A127*, 1949.

[6] C. J. Stairmand. The design and performance of cyclone separators. *Industrial and Engineering Chemistry*, 29:356–383, 1951.

[7] W. Barth. Design and layout of the cyclone separator on the basis of new investigations. *Brennstow-Wäerme-Kraft (BWK)*, 8(4):1–9, 1956.

[8] A. Avci and I. Karagoz. Theoretical investigation of pressure losses in cyclone separators. *International Communications in Heat and Mass Transfer*, 28(1):107–117, 1 2001.

[9] B. Zhao. A theoretical approach to pressure drop across cyclone separators. *Chemical Engineering Technology*, 27:1105–1108, 2004.

[10] I. Karagoz and A. Avci. Modelling of the pressure drop in tangential inlet cyclone separators. *Aerosol Science and Technology*, 39(9):857–865, 2005.

[11] J. Chen and M. Shi. A universal model to calculate cyclone pressure drop. *Powder Technology*, 171(3):184 – 191, 2007.

[12] J. Casal and J. M. Martinez-Benet. A better way to calculate cyclone pressure drop. *Chemical Engineering*, 90(2):99–100, 1983.

[13] J. Dirgo. *Relationship between cyclone dimensions and performance*. PhD thesis, Harvard University, USA, 1988.

[14] J. Gimbun, T.G. Chuah, A. Fakhru'l-Razi, and T. S. Y. Choong. The influence of temperature and inlet velocity on cyclone pressure drop: a cfd study. *Chemical Engineering & Processing*, 44(1):7–12, 2005.

[15] H. Safikhani, M.A. Akhavan-Behabadi, M. Shams, and M. H. Rahimyan. Numerical simulation of flow field in three types of standard cyclone separators. *in press Advanced Powder Technology*, 2010.

[16] C. J. Stairmand. Pressure drops in cyclone separators. *Industrial and Engineering Chemistry*, 16(B):409–411, 1949.

[17] Alex C Hoffmann and Louise E Stein. *Gas cyclones and swirl tubes principle, design and operation*. Springer, second edition, 2008.

[18] E. Muschelknautz and M. Trefz. Design and calculation of higher and design and calculation of higher and highest loaded gas cyclones. *in 'Proceedings of Second World Congress on Particle Technology' Kyoto, Japan*, pages 52–71, October 1990.

[19] E. Muschelknautz and M. Trefz. VDI-Wärmeatlas. *Druckverlust und Abscheidegrad in Zyklonen*, 6 Auflage:Lj1 – Lj9, 1991.

[20] E. Muschelknautz and W. Kambrock. Aerodynamische beiwerte des zyclon abscheiders aufgrund neuer und verbesserter messungen. *Chem-Ing-Tech*, 42(5):247–55, Chemie Ingenieur Technik 1970.

[21] E. Muschelknautz. Die berechnung von zyklonabscheidern fur gas. *Chemie Ingenieur Technik*, 44:63–71, 1972.

[22] M. Trefz. Die vershiedenen abscheidevorgange im hoher un hoch beladenen gaszyklon unter besonderer berucksichtigung der sekundarstromung. *Forschritt-Berichte VDI; VDI-Verlag GmbH: Dusseldorf, Germany*, 295, 1992.

[23] M. Trefz and E. Muschelknautz. Extended cyclone theory for gas flows with high solids concentrations. *Chemie Ingenieur Technik*, 16:153–160, 1993.

[24] C. Cortés and A. Gil. Modeling the gas and particle flow inside cyclone separators. *Progress in Energy and Combustion Science*, 33(5):409 – 452, 2007.

[25] J. S. Cowpe, J. S. Astin, R. D. Pilkington, and A. E. Hill. Application of response surface methodology to laser-induced breakdown spectroscopy: Influences of hardware configuration. *Spectrochimica Acta Part B*, 62:1335 – 1342, 2007.

[26] G. E. P. Box and K. B. Wilson. On the experimental attainment of optimum conditions. *Journal of the Royal Statistical Society*, 13:1–45, 1951.

[27] P. O. Haaland. *Experimental design in biotechnology*. Marcel Dekker, New York, 1989.

[28] R. H. Myers and D. C. Montgomery. *Response surface methodology: Process and product optimization using designed experiments*. Wiley, New York, 2 edition, 2002.

[29] C. Liyana-Pathirana and F. Shahidi. Optimization of extraction of phenolic compounds from wheat using response surface methodology. *Food Chemistry*, 93:47–56, 2005.

[30] Y. Yuan, Y. Gao, L. Mao, and J. Zhao. Optimisation of conditions for the preparation of β-carotene nanoemulsions using response surface methodology. *Food Chemistry*, 107:1300–1306, 2008.

[31] M. Gfrerer and E. Lankmayr. Screening, optimization and validation of microwave-assisted extraction for the determination of persistent organochlorine pesticides. *Analytica Chimica Acta*, 533:203–211, 2005.

[32] J. A. Nelder and R. Mead. A simplex method for function minimization. *The Computer Journal*, 7(4), 1965.

[33] Wikipedia. Nelder-mead method. URL `http://en.wikipedia.org/wiki/NelderMead_method`.

[34] W. H. Press, B. P. Flannery, S. A. Teukolsky, and W. T. Vetterling. *Numerical Recipes in FORTRAN 77: The Art of Scientific Computing*. Cambridge University Press, Cambridge, UK, 1992.

[35] W. D. Griffiths and F. Boysan. Computational fluid dynamics (cfd) and empirical modelling of the performance of a number of cyclone samplers. *Journal of Aerosol Science*, 27(2):281–304, 1996.

[36] T.G. Chuah, J. Gimbun, and Thomas S.Y. Choong. A cfd study of the effect of cone dimensions on sampling aerocyclones performance and hydrodynamics. *Powder Technology*, 162:126 – 132, 2006.

[37] M. D. Slack, R. O. Prasad, A. Bakker, and F. Boysan. Advances in cyclone modeling using unstructured grids. *Trans IChemE.*, 78 Part A, (2000), 2000.

[38] A. J. Hoekstra. *Gas flow field and collection efficiency of cyclone separators*. PhD thesis, Technical University Delft, 2000.

[39] A. Horvath, C. Jordan, and M. Harasek. Influence of vortex-finder diameter on axial gas flow in simple cyclone. *Chemical Product and Process Modeling*, 3(1), 2008.

[40] S. A. Morsi and A. J. Alexander. An investigation of particle trajectories in two-phase flow systems. *Journal of Fluid Mechanics*, 55(02):193–208, 1972.